



## Vacancy–solute complexes in aluminum

O. Melikhova\*, J. Kuriplach, J. Čížek, I. Procházka

*Department of Low Temperature Physics, Faculty of Mathematics and Physics,  
Charles University, V Holešovičkách 2, CZ-18000 Prague, Czech Republic*

Available online 4 October 2005

### Abstract

Several vacancy–solute complexes in the Al matrix are examined theoretically. In particular, these are V–Cu, V–Cd, V–In, V–Sn, V–Si and V–Fe. We concentrate on coincidence Doppler broadening (high momentum) profiles and positron lifetimes that bring complementary information about these defects. Positron calculations are carried out utilizing the atomic superposition method employing realistic atomic configurations obtained using an ab initio pseudopotential method. In this study we inspect to what extent such defects are detectable and differentiable using positron annihilation techniques. The influence of lattice relaxations around defects on the positron properties turns out to be important and is also debated. The obtained results are discussed in connection with experimental data published in literature.

© 2005 Elsevier B.V. All rights reserved.

**Keywords:** Aluminum alloys; Vacancy–solute complexes; Electron–positron momentum distribution; Atomic superposition method; Lattice relaxations

### 1. Introduction

Aluminum is the second most widely used metal in industry and the most wrought aluminum alloys are strengthened by age-hardening. Principle of age-hardening is controlling mechanical properties of an alloy by regulating the decomposition of the super-saturated solid solution (SSS) of solute elements in the matrix. One of the age-hardening alloy systems is Al–Cu, which serves as a basis for commercial 2xxx alloy

series. The complete decomposition sequence in this alloy is: SSS–GP zones– $\theta''$ – $\theta'$ – $\theta$ . Maximum hardening occurs if there is present a critical dispersion of GP zones, or an intermediate precipitates, or both. Trace additions of Cd, In, and Sn increase both the rate and extent of hardening in Al–Cu alloys aged at temperatures between 100 and 200 °C [1]. These elements suppress the formation of the GP zones and  $\theta''$  phase and stimulate a finer and more uniform dispersion of the semicoherent  $\theta'$  phase. Such a behavior was explained in terms of the so-called vacancy trapping effect proposed by Kimura and Hasiguti [2] suggesting that these microalloying atoms bind vacancies that would be otherwise available for Cu diffusion.

\* Corresponding author. Tel.: +420 22191 2788;

fax: +420 22191 2567.

E-mail address: [oksivmel@yahoo.com](mailto:oksivmel@yahoo.com) (O. Melikhova).

Studying properties of vacancy–solute complexes is of primary importance in order to understand vacancy-assisted processes taking part in such alloys [3]. In particular, the exchanges of a vacancy and a neighboring solute atom promote the diffusion of vacancy–solute complexes and the precipitation of solute atoms. Positron annihilation (PA) spectroscopy and especially coincidence Doppler broadening (CDB) spectroscopy may contribute significantly when studying vacancy–solute complexes. The sensitivity of CDB to chemical surrounding of positron traps allows us to observe directly the presence of a solute element in the vicinity of a vacancy.

The present study is aimed at the theoretical calculations of positron lifetimes and the so-called high momentum parts (HMPs) of CDB profiles for the vacancy complexes with the solute atoms mentioned above. Relaxations around a defect, vacancy–solute binding energies ( $E_b$ ) and positron-defect binding energies ( $E_{pb}$ ) are also calculated. In addition to microalloying elements, results for complexes with Si and Fe, which are the often-encountered impurities in Al-based alloys, are also provided in order to separate their effect on PA results. Such theoretical calculations can be very helpful when interpreting PA measurements carried out on Al–Cu based alloys and identifying open volume defects seen by positrons. This was recently demonstrated in our study of an Al–Sn alloy [4].

## 2. Computational methods

Relaxed atomic configurations of the studied complexes and monovacancy in Al were obtained

using the Vienna ab initio simulation package (VASP) [5] developed at the Institute für Materialphysik of the Universität Wien employing the ultrasoft pseudopotentials [6] supplied with the package. In these calculations 108 atom-based supercells ( $3 \times 3 \times 3$  fcc cell of Al) were used. The monovacancy was created by removing one Al atom. In order to form the vacancy–solute complex, an Al atom in the nearest neighborhood of the vacancy was replaced by a solute atom. The total energy of the supercell was then minimized with respect to atomic positions (see [5] for details) within the local density approximation framework [7]. In all calculations we used 8  $k$ -points in the Brillouin zone (BZ). The plane wave cut-off energy was 235 eV. In order to have an idea of binding energies ( $E_b$ ) of vacancy–solute complexes, we also calculated the total energy ( $E_S$ ) of the configuration with a single solute atom. Then:

$$E_b = E_V + E_S - (E_{V+S} + E_{Al}) \quad (1)$$

where  $E_V$ ,  $E_{V+S}$  and  $E_{Al}$ , are respectively, energies of supercells corresponding to the monovacancy, vacancy–solute complex and Al bulk. We should mention, however, that binding energies presented below should be considered as preliminary only because their convergence with respect to the BZ sampling needs to be yet checked.

Positron calculations were carried out employing the so-called atomic superposition (ATSUP) method [8]. In these calculations we used 500 atom supercells obtained from those used in VASP calculations by adding additional atoms at the sides of these supercells. Such added atoms were arranged in the form of the regular Al fcc lattice. The scheme described in [9] was utilized for calculations of high momentum parts

Table 1

Basic information about the studied complexes and matrix: core electron configuration, atomic volume ( $\Omega_0$ ), relaxation around defects, vacancy–solute binding energies ( $E_b$ ) – calculated value and the range of values from those referred to in [15] (the average value is given in parentheses)

Complex	Core configuration	$\Omega_0$ ( $\text{\AA}^3$ )	Relaxations (%) S; Snn; Vnn; Onn	$E_b$ (eV) calculation	$E_b$ (eV) literature
V	(Ne)	16.6	–; –; +0.7; –	–	–
V–Cu	(Ar) + 3d <sup>10</sup>	11.8	–2.9; +1.1; +0.8; +2.5 (S)	0.06	0.05–0.29 (0.19)
V–Cd	(Kr) + 4d <sup>10</sup>	21.8	+4.2; –1.4; +0.8; –1.8 (S)	0.18	0.18–0.32 (0.25)
V–In	(Kr) + 4d <sup>10</sup>	26.1	+4.9; –1.9; +0.7; –2.5 (S)	0.19	0.18–0.39 (0.27)
V–Sn	(Kr) + 4d <sup>10</sup>	27.1	+5.0; –2.2; +0.8; –2.8 (S)	0.20	0.22–0.46 (0.38)
V–Si	(Ne)	20.1	+0.9; +0.6; +0.8; +1.7 (V)	0.04	0.12–0.31 (0.24)
V–Fe	(Ar) + 3d <sup>6</sup>	11.8	–4.4; +2.7; +1.0; +6.3 (S)	0.13	0.18

Relaxations are given in % of the Al lattice constant. The explanation of symbols S, Snn, Vnn, Onn and V is given in the text.

(HMPs) of the momentum distribution of annihilation photons. The range  $(15 - 25) \times 10^{-3} m_e c$  was used in calculations of the  $W$ -parameter. The calculated spectra were convoluted with a Gaussian function with the width 1 keV ( $=3.91 \times 10^{-3} m_e c$ ; full width at half maximum), which corresponds to a typical experimental energy resolution of CDB spectrometers. Core electron configurations for all atomic species are specified in Table 1. However, in the case of atoms with d-electrons it may be necessary to reduce the number of d-electrons considered in HMP calculations to reproduce well experimental CDB profiles (see e.g. [10]). This correction is neglected in the present work. In lifetime calculations electron–positron correlations were treated according to Boroński and Niemenen [11], whereas a gradient-correction scheme of Barbiellini et al. [12] was employed in HMP calculations. We further refer to [13,14] for details concerning theoretical approaches and related computational procedures used in positron solid-state physics.

### 3. Results and discussions

We discuss first non-positron results, i.e. relaxations and vacancy–solute binding energies. As for relaxations (see Table 1), we found that it is reasonable to divide the first nearest neighbors (nns) of vacancy–solute complexes into three classes. These are: the first nns of the solute atom that are not the first nns of the vacancy (we label them further as Snn), in the same sense we consider the first nns of the vacancy (Vnn), and other atoms which are simultaneously the first nns of both the solute atom and the vacancy (Onn). Within these classes the relaxations are usually of the same character with respect to the solute atom (Snn) or vacancy (Vnn); the direction of relaxation is marked by the ‘–’ sign and ‘+’ sign for outward and inward relaxations, respectively. In the case of Onns the situation is somewhat mixed and the dominant shift is given (S (V) means with respect to the solute atom (vacancy)). The direction of the relaxation of the solute atom is given in terms of the shift with respect to the vacancy considering the same sign convention as above. In Table 1, relaxations of the maximum amplitude for S, Snn, Vnn, and Onn cases are listed.

Roughly speaking, the magnitude of relaxations increases as the deviation of the solute and Al atomic

volumes increases (see Table 1). Relaxations around vacancy (Vnns) are very similar to those found around non-decorated vacancy in Al and are always inward. Concerning other types of relaxations, in principle, we can define three groups of solute atoms. First, Si–vacancy pairs exhibit rather small relaxations whose magnitudes are mostly less than 1% and are always inward. Second, Cu and Fe vacancy complexes show strong outward relaxations for the solute atoms, whereas Snn and Onn relaxations are inward. Note that Cu and Fe are both 3d atoms. Third, V–Cd, V–In and V–Sn complexes display relaxations that are just opposite to the previous case concerning directions. For all these atoms, 4d electrons belong to outermost electrons. The difference between the second and third class of atoms can be perhaps explained in terms of the atomic volume. The 3d atoms – with the atomic volume smaller than for Al – are tightly bound to surrounding Al atoms and are thus pushed away from the vacancy. In contrast to this, 4d atoms move towards the vacancy in order to find more space for themselves because their atomic volume is bigger than that for the matrix atoms.

In the fifth column of Table 1 we specify calculated binding energies of studied vacancy–solute complexes. The vacancy–solute binding energies reported in literature [15] exhibit a wide range of values (the sixth column of Table 1), so it is difficult to come to a definitive conclusion about precise values. We consider here the average of values listed in [15] (further referred to as ‘averaged values’) as the most probable values for vacancy–solute binding energies. Then, the calculated values for V–Cd, V–In, V–Sn and V–Fe complexes are in acceptable agreement with averaged ones. However, the calculated  $E_b$  values for V–Cu and V–Si are apparently lower than averaged ones. Nevertheless, both calculated and averaged values of  $E_b$ ’s for V–Cd, V–In and V–Sn complexes are higher than that for V–Cu, which is in agreement with the vacancy trapping model mentioned above. The energies for V–Si and V–Fe can be considered as about the same or lower compared to V–Cu, which is supported by the fact that Si and Fe atoms do not influence significantly the precipitation of Cu [16].

We now continue with positron characteristics. Calculated positron lifetimes ( $\tau$ ),  $W$ -parameters and positron binding energies ( $E_{pb}$ ) to defects are listed in Table 2. Results for both relaxed and non-relaxed

Table 2  
Results of positron calculations for bulk Al, monovacancy in Al and studied vacancy-solute complexes in Al

Complex	$\tau$ (ps)	100 W	$E_{pb}$ (eV)
Bulk	168	0.509	–
V	239 (244)	0.208 (0.196)	1.92 (2.13)
V–Cu	235 (242)	0.377 (0.410)	1.99 (2.32)
V–Cd	235 (240)	0.323 (0.288)	2.12 (2.33)
V–In	237 (241)	0.277 (0.249)	2.01 (2.11)
V–Sn	236 (241)	0.253 (0.229)	1.98 (2.09)
V–Si	236 (243)	0.208 (0.191)	1.88 (2.20)
V–Fe	229 (243)	0.270 (0.272)	1.56 (2.21)

Results for non-relaxed configurations are given in parentheses.

configurations are shown. The calculated value for the single vacancy agrees well with other calculations and also with experiment (see [4] and references therein). In any case the positron lifetime of the monovacancy is not significantly influenced by the presence of the solute atom (except perhaps iron) and this characteristics can hardly be used to identify and/or distinguish among complexes. Furthermore, one can see that lifetimes and binding energies are always reduced due to relaxations, which is caused by the fact that the size of the corresponding free volume is reduced – that also lowers the depth of the positron potential well – as relaxations of Al atoms around the vacancy (Vnns) are always inward. S, Onn and Snn relaxations play only a minor role (the only exception appears to be Fe).

In the case of  $W$ -parameter the situation turns out to be more complicated. For the monovacancy, the value of  $W$  slightly increases due to (inward) relaxations as the overlap with neighboring atoms also increases. Except for Si, the addition of a solute atom increases the  $W$ -parameter, and d-electrons are responsible for this effect. If the relaxation of the solute atom is outward (Fe and Cu, Table 1), the effect of the reduction of the overlap with this atom can have a stronger influence than inward relaxations of Vnns and, consequently, the  $W$ -parameter decreases. In other cases the  $W$ -parameter is increased after relaxation.

On the other hand, measuring the  $W$ -parameter and high momentum profiles, in general, constitutes the basis for the identification of vacancy-solute complexes. This is demonstrated in Fig. 1 where ratio high momentum profiles are shown. The ratio profiles are made with respect to defect free Al. Before we start the

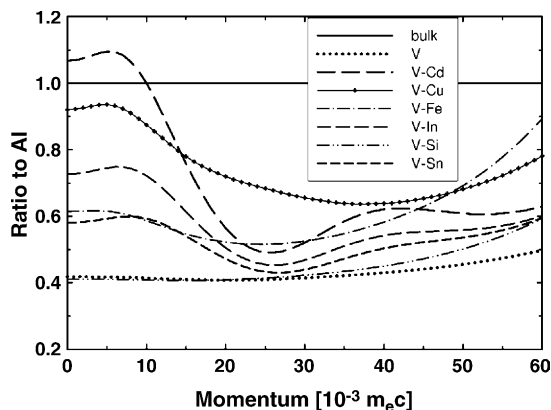


Fig. 1. High momentum ratio profiles (with respect to defect free Al) for the monovacancy in Al and studied vacancy-solute complexes. The curves correspond to relaxed configurations.

discussion about these profiles, we should mention that profiles do not contain the contribution from valence electrons and a comparison with experiment is meaningful only for momenta higher than about  $15 \times 10^{-3} m_e c$ . Furthermore, here we make plots up to  $60 \times 10^{-3} m_e c$ , but the region up to  $40 \times 10^{-3} m_e c$  is usually experimentally accessible.

As seen in Fig. 1, we can clearly define several groups of complexes with respect to their HMP response. First, the V–Si complex exhibits behavior that is very close to that of the monovacancy and these two defects are therefore hardly mutually differentiable. Second, V–Cd, V–In and V–Sn complexes create the second group that can be well distinguished from other complexes. The characteristic feature is the well-pronounced minimum at about  $25 \times 10^{-3} m_e c$  (see also [4]). Third, in contrast to the second group the profile of V–Fe shows only very shallow minimum that is shifted to lower momenta. Fourth, V–Cu itself constitutes the last group that exhibits a characteristic behavior with a minimum around  $40 \times 10^{-3} m_e c$  and an amplitude that is positioned apparently higher than profiles for other complexes. This should make V–Cu well differentiable from other complexes.

In order to show the influence of lattice relaxations on HMP profiles, in Fig. 2, we present ratio profiles for non-relaxed configurations of complexes. One can see that the main effect of relaxations on HMP profiles is an accentuation of minima. In the case of V–Fe and V–Cu there are even no minima in non-relaxed profiles.

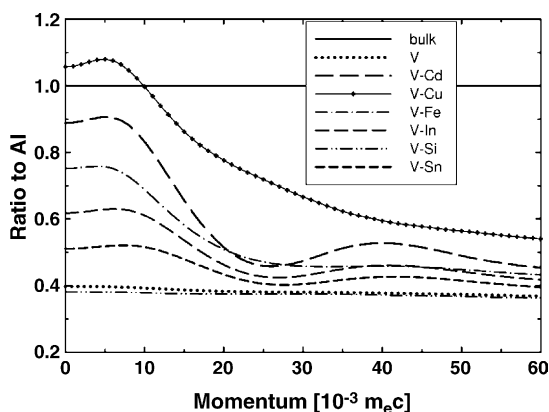


Fig. 2. High momentum ratio profiles (with respect to defect free Al) for the monovacancy in Al and studied vacancy–solute complexes. The curves correspond to non-relaxed configurations.

This clearly shows that lattice relaxations should be considered in calculations of HMP profiles.

In our recent work [4], we studied an Al–Sn alloy using a CDB spectrometer. We could clearly identify the V–Sn complex present in the as-quenched specimen. The measured ratio profile agreed well with the calculated one though it was slightly shifted towards higher values (see Fig. 8 in [4]). To our knowledge, except for V–Sn the vacancy–solute complexes studied here were not yet directly investigated by the CDB technique. However, there have been many other investigations of Al-based alloys using this technique. For instance, Nagai et al. [17] studied a quenched Al–Cu alloy. The defect CDB ratio profile is not extracted and, thus, we cannot compare it with the calculated profile presented in this work. The same holds for the study by Somoza et al. [18]. Other more complicated Al-based alloys were investigated using CDB, e.g. in [17–20].

In conclusion, we can state that PA can supply direct information about vacancy–solute complexes in Al–Cu-based alloys. From the results of calculations reported in this work we can see that it is possible to distinguish between vacancies bound to Cu atoms and vacancies bound to microalloying elements Cd, In and Sn as well as vacancies bound to Si and Fe, which are common impurities in commercial Al alloys. This can be very useful for interpretation of experimental PA results and better understanding of the precipitation

processes in the commercial Al alloys at the microscopic level.

## Acknowledgements

We are grateful to M.J. Puska for his ATSUP code that served as a basis for further developments. This work is a part of the research plan MS 0021620834 that is financed by the Ministry of Education of the Czech Republic.

## References

- [1] S.P. Ringer, K. Hono, *Mater. Character.* 44 (2000) 101.
- [2] H. Kimura, R.R. Hasiguti, *Acta Metall.* 9 (1961) 1076.
- [3] I. Polmear, *Mater. Sci. Forum* 363–365 (2001) 1.
- [4] J. Čížek, O. Melikhova, I. Procházka, J. Kuriplach, I. Stulíková, P. Vostrý, J. Faltus, *Phys. Rev. B* 71 (2005) 064106.
- [5] G. Kresse, J. Hafner, *Phys. Rev. B* 47 (1993) 558; G. Kresse, J. Hafner, *Phys. Rev. B* 49 (1994) 14251; G. Kresse, J. Furthmüller, *Comput. Mater. Sci.* 6 (1996) 15; G. Kresse, J. Furthmüller, *Phys. Rev. B* 54 (1996) 11169.
- [6] G. Kresse, J. Hafner, *J. Phys.: Condens. Matter* 6 (1994) 8245.
- [7] D.M. Ceperley, B.J. Alder, *Phys. Rev. Lett.* 45 (1980) 566; J.P. Perdew, A. Zunger, *Phys. Rev. B* 23 (1981) 5048.
- [8] M.J. Puska, R.M. Nieminen, *J. Phys. F: Met. Phys.* 13 (1983) 333; A.P. Seitsonen, M.J. Puska, R.M. Nieminen, *Phys. Rev. B* 51 (1995) 14057.
- [9] J. Kuriplach, A.L. Morales, C. Dauwe, D. Segers, M. Šob, *Phys. Rev. B* 58 (1998) 10475.
- [10] E. Dryzek, J. Kuriplach, J. Dryzek, *J. Phys.: Condens. Matter* 10 (1998) 6573.
- [11] E. Boroński, R.M. Nieminen, *Phys. Rev. B* 34 (1986) 3820.
- [12] B. Barbiellini, M.J. Puska, T. Torsti, R.M. Nieminen, *Phys. Rev. B* 51 (1995) 7341.
- [13] M.J. Puska, R.M. Nieminen, *Rev. Mod. Phys.* 66 (1994) 841.
- [14] J. Kuriplach, *Appl. Surf. Sci.* 194 (2002) 61.
- [15] L.F. Mondolfo, *Aluminum Alloys: Structure and Properties*, Butterworths, London, 1976, p. 24.
- [16] L.F. Mondolfo, *Aluminum Alloys: Structure and Properties*, Butterworths, London, 1976, p. 265.
- [17] Y. Nagai, M. Murayama, Z. Tang, T. Nonaka, K. Hono, M. Hasegawa, *Acta Mater.* 49 (2001) 913.
- [18] A. Somoza, M.P. Petkov, K.G. Lynn, A. Dupasquier, *Phys. Rev. B* 65 (2002) 094107.
- [19] M. Biasini, G. Ferro, P. Folegati, G. Riontino, *Phys. Rev. B* 63 (2001) 092202.
- [20] T. Honma, S. Yanagita, K. Hono, Y. Nagai, M. Hasegawa, *Acta Mater.* 52 (2004) 1997.